FOODBORNE PATHOGENS AND DISEASE
Volume 00, Number 00, 2024

DOI: 10.1089/fpd.2024.0025



# Preparation and Keep-Refreshing Effect of Chitosan/Sea Buckthorn Polysaccharide Composite Film on the Preservation of Yellow Cherry Tomatoes

Miaorong Xiao,[1,*] Ao Shen,[1,*] Xiaodi Chen,[1] Tongtong Lu,[1] Jin Zhang,[1] Shuzhen Li,[2] and Weiwei Yang[1]

**Abstract**

In this study, sea buckthorn polysaccharides (SBP) were added as functional substances to chitosan (CS), and chitosan/sea buckthorn polysaccharide (SCS) composite films were prepared using the casting method. The effects of SBP addition on the optical properties, physical properties, mechanical properties, structure, antioxidant activity, and antibacterial activity of the SCS composite films were studied, and the prepared SCS composite films were used to preserve yellow cherry tomatoes. The results showed that SCS composite films exhibited good UV resistance, water solubility, and antioxidant activity, but its apparent structure, hydrophobicity, and mechanical properties needed further improvement. Meanwhile, SBP has inhibitory effects on all 8 experimental strains. In addition, the SCS composite film with the addition of 200 mg/L SBP could reduce the weight loss rate of yellow cherry tomatoes, maintain hardness, delay the decrease of total soluble solids, titratable acid, and Vitamin C content, and inhibit the accumulation of malondialdehyde. SCS composite films are beneficial for enhancing the quality of yellow cherry tomatoes during storage, and their application in fruit and vegetable preservation has development prospects.

**Keywords:** sea buckthorn polysaccharide, chitosan, film, yellow cherry tomatoes, preservation

## Introduction

Chitosan (CS) exhibits potential as a novel material for preserving freshness due to its film-forming capabilities and antioxidant properties (Shariatinia, 2018). Nonetheless, the efficacy of pure CS films is somewhat constrained by the large molecular size of CS, which hampers its interaction with food spoilage agents (Liu et al., 2017, Narasagoudr et al., 2020). Previous studies have shown that films created from a combination of polysaccharides and CS possess superior mechanical properties and demonstrate enhanced antioxidant and antibacterial activities (Al-Hilifi et al., 2024, Al-Hilifi et al., 2023, Kumar et al., 2020). This synergistic improvement addresses the performance limitations of single-component films (Kumar et al., 2021, Sun et al., 2022, Zhao et al., 2023).

Sea buckthorn polysaccharides (SBP) are recognized for their diverse biological activities, including antioxidant, antibacterial, and antifatigue effects (Li et al., 2024, Liu et al., 2021, Shen et al., 2021). Despite their potential, research on applying SBP to the fabrication of composite films remains scant.

The substantial biological activities of SBP and CS underpin their application in extending the shelf life of yellow cherry tomatoes through the development of novel preservation strategies. This research utilizes CS and SBP as primary materials to engineer composite films aimed at enhancing perishable food packaging. Our objectives are to meticulously assess the mechanical, physicochemical, and structural attributes of the films and to explore the efficacy of these SBP-enriched SCS films in preserving yellow cherry tomatoes. This study strives to advance sustainable

[1]Department of Food Science, College of Public Health, Shenyang Medical College, Shenyang, China.
[2]Department of Immunology, College of Basic Medical Sciences, Shenyang Medical College, Shenyang, China.
*These authors contributed equally to this work.

packaging solutions that significantly prolong the shelf life of perishable products.

## Materials and Methods

### Materials and reagents

Yellow cherry tomatoes (variety: Huang guan). Purchased from a local farm in Shenyang, China. SBP (50% purity): Obtained from Xi'an Michel Biotechnology Co., Ltd. (Xi'an, China). CS: Purchased from Waters Biotechnology Co., Ltd. (Lanzhou, China). Chemicals: Anhydrous oxalic acid was acquired from McLean Biochemical Technology Co., Ltd. (Shanghai, China). Other reagents and chemicals are analytical grade reagents.

### Preparation of the SCS composite film

A solution was prepared by adding 1 mL of glycerol to 100 mL of 2% (v/v) acetic acid solution, followed by vigorous stirring using a magnetic stirrer. Subsequently, 3 g of CS was thoroughly dissolved in this mixture. Different concentrations of SBP (0 mg, 50 mg, 100 mg, 150 mg, 200 mg) were then introduced, and the mixture was subjected to ultrasonic treatment at room temperature for 25 min to eliminate air bubbles. The resultant solution was cast onto a customized 25 cm × 25 cm glass plate and dried in an oven at 60°C for 6 h to form the composite films designated as CS, SCS-I, SCS-II, SCS-III, and SCS-IV. Before further analysis, the films were conditioned in an environment maintained at 25°C and 60% relative humidity for over 24 h.

### Optical properties test

The color parameters of the samples were measured using a portable colorimeter, focusing on $L$ (brightness), $a$ (redness/greenness), and $b$ (yellowness/blueness). Calibration was conducted against black-and-white standards before the measurements were taken at the center of each sample. The total color difference ($\Delta E$) was calculated based on the color values for standard whiteboards ($L_0$ = 93.28, $a_0$ = −1.1, $b_0$ = −1.3) (Kaczmarek-Szczepańska et al., 2022).

$$\Delta E = \sqrt{(L - L_0)^2 + (a - a_0)^2 + (b - b_0)^2}$$

The transmittance of the films was assessed to evaluate the optical properties further. Samples were cut into rectangles (10 × 40 mm) and placed in a colorimetric dish. The transmittance across a 200–800 nm wavelength range was measured (Bai et al., 2020, Roy and Rhim, 2020).

### Physical properties test

Samples (20 × 20 mm) were first dehydrated at 105°C for 24 h until a constant weight was achieved (denoted as $m_1$). These dried films were then immersed in 50 mL of distilled water, sealed with cling film to prevent evaporation, and stored at 25°C for 24 h. Surface moisture was carefully removed after immersion, and the wet samples were weighed ($m_2$). Subsequently, the rehydrated films were dried again under the initial conditions, and their final weight was recorded as $m_3$.

$$SD\,(\%) = \frac{m_2 - m_1}{m_1} \times 100$$

$$WS\,(\%) = \frac{m_1 - m_3}{m_1} \times 100$$

Water vapor permeability (WVP) was determined following the method described by Wu et al. (2023), with minor modifications. A small bottle containing 100 mL of distilled water was sealed with the film under test and placed in a desiccator with anhydrous silica gel at 25°C (Marangoni Júnior et al., 2022). The combined weight of the small bottle and film was measured at intervals of 0 h, 8 h, 16 h, and 24 h. The WVP value was calculated using the formula provided, where $G$ is the weight of the small bottle and film in grams, $L$ is the film thickness in meters, $t$ is the time interval in seconds, $s$ is the surface area of the bottle mouth, and $\Delta p$ is the water vapor pressure difference across the film (3168 Pa at 25°C).

$$WVP = \frac{G \times L}{t \times s \times \Delta p}$$

### Thickness and mechanical properties testing

Film thickness was measured using a digital micrometer with a precision of 0.001 mm. Measurements were made at 10 randomly chosen points on each film, with each set of measurements replicated thrice. For the assessment of mechanical properties, film strips measuring 100 × 10 mm were subjected to tensile strength (TS) and elongation at break (EAB) tests. These tests were performed at a stretching speed of 100 mm/min, and each sample group was tested in five replicates (Wu et al., 2023, Zhao et al., 2023).

### Structural properties

Attenuated total reflectance Fourier transform infrared spectroscopy. The chemical structure of the films was analyzed using an attenuated total reflectance Fourier transform infrared spectrometer (Nicolet iS10, Thermo Fisher Scientific, United States). For each sample, 64 scans were collected over a wavelength range of 4000 to 400 $cm^{-1}$ at a resolution of 8 $cm^{-1}$.

### Scanning electron microscopy

The surface and cross-sectional microstructure of the films were examined via scanning electron microscopy (SEM) (Gemini 500, Carl Zeiss AG, Germany). Observations were conducted at an acceleration voltage of 2 kV and a magnification of 16 kX.

### DPPH free radical scavenging activity

A 0.1 mmol/L DPPH ethanol solution (3 mL) was mixed with 750 μL of the liquid sample and vortexed. A measure of 750 μL of 2% acetic acid was mixed with 3 mL of the DPPH ethanol solution for the control. Both the sample and control were incubated in the dark for 30 min. The absorbance was measured at 517 nm. The percentage of DPPH radical scavenging activity (RSA) was calculated

using the below equation, where $A_c$ represents the control's absorbance and $A_s$ represents the sample's absorbance.

$$RSA\,(\%) = \frac{A_c - A_s}{A_s} \times 100$$

### Antimicrobial activity

Following the methodology outlined in previous research (Shen et al., 2023), the diameter of the inhibition zone and the minimum inhibitory concentration (MIC) of eight strains were determined (Table 1 and Table 2).

### Determination of the preservation effect of composite cling film on yellow cherry tomatoes

Weight loss rate. The initial weight of yellow cherry tomatoes was recorded as $m_0$ (g) on day 0. Subsequent weights were measured on days 4, 8, 12, and 16 as $m_t$ (g). The experiments were organized into three replicates per sample group.

$$Weight\ loss\ rate\,(\%) = \frac{m_0 - m_t}{m_0} \times 100$$

### Hardness

The hardness of yellow cherry tomatoes was measured using a GY-4-J digital fruit hardness tester. The tester, equipped with a 3-mm-diameter probe, was applied perpendicularly to the tomato surface and pressed in at a uniform speed of 10 mm/s to a depth of 10 mm. Measurements were taken at three different points on each tomato to calculate an average value expressed in Newtons.

### Total soluble solids

Five grams of fruit was centrifuged at 4,000 rpm for 10 min. The total soluble solid (TSS) content was then measured using an Abbe refractometer.

### Titratable acid

A 10 g sample of yellow cherry tomato tissue was homogenized and diluted with distilled water to a final volume of 100, resting for 30 min. A 20 mL filtrate was taken, and 2 drops of 1% phenolphthalein indicator were added. Titration was performed using a 0.1 M sodium hydroxide (NaOH) solution until the persistent color change was noted. A control titration was conducted with distilled water in place of the sample filtrate. The titrable acid (TA) content was calculated using the malic acid conversion coefficient (0.067) using the following formula:

$$TA\,(\%) = \frac{V \times c \times (V_1 - V_0) \times f}{V_s \times m} \times 100$$

Where $V$ represents the total volume of sample extraction solution (mL), $V_S$ is the volume of filtrate taken for titration (mL), $c$ is the concentration of NaOH titrant (mol $L^{-1}$), $V_1$ is the volume of NaOH solution consumed by the sample filtrate (mL), $V_0$ is the volume consumed for the control titration (mL), and $m$ is the weight of the sample (g).

### Vitamin C content

The vitamin C (VC) content in yellow cherry tomatoes was quantified using the 2,6-dichlorophenol indophenol titration method, as described by Zhao et al. (2023). In this method, $V$ represents the total volume of the yellow cherry tomato extract (in mL); $V_3$ is the volume of titration for the yellow cherry tomato extract (in mL); $V_2$ denotes the volume of 2,6-dichloroindophenol consumed during the oxalic acid titration (in mL); $\rho$ is the mass of 1 mL of 2,6-dichloroindophenol equivalent to VC (in mg/mL); $V_4$ is the volume of the sample extract used for titration (mL); and m is the mass of 2,6-dichloroindophenol consumed by the yellow cherry tomatoes (g).

$$VC = \frac{\mathrm{V} \times (V_3 - V_2) \times \rho}{\mathrm{m} \times V_4} \times 100$$

### Malondialdehyde content

One gram of fruit sample was homogenized with 5 mL of 10% (w/v) trichloroacetic acid (TCA) and centrifuged

Table 1. Antibacterial Activity of SBP Solutions and Film Solutions

| | | *Inhibition Zone Diameter (mm)* | | | | | |
|---|---|---|---|---|---|---|---|
| | | *SBP Solutions* | | *SBP Film Solutions* | | | |
| *No.* | *Strain* | *0.5* | *1.0* | *0.5* | *1.0* | *PC* | *NC* |
| 1 | *Escherichia coli* | $8.33 \pm 0.55^{ab}$ | $9.76 \pm 0.29$ | $8.42 \pm 0.36^{ab}$ | $9.82 \pm 0.28$ | $10.17 \pm 0.26$ | – |
| 2 | *Pseudomonas aeruginosa* | $8.28 \pm 0.79^{ab}$ | $9.18 \pm 0.78$ | $8.77 \pm 0.63^{ab}$ | $9.29 \pm 0.57$ | $9.72 \pm 0.20$ | – |
| 3 | *Bacillus subtilis* | $7.36 \pm 0.19^{ab}$ | $8.36 \pm 0.06$ | $7.24 \pm 0.26^{ab}$ | $8.54 \pm 0.68$ | $9.58 \pm 0.38$ | – |
| 4 | *Bacillus cereus* | $7.91 \pm 0.29^{ab}$ | $8.82 \pm 0.61$ | $8.04 \pm 0.45^{ab}$ | $8.87 \pm 0.24$ | $9.72 \pm 0.09$ | – |
| 5 | *Aspergillus flavus* | $9.08 \pm 0.18^{ab}$ | $9.88 \pm 0.85^{b}$ | $9.36 \pm 0.49^{ab}$ | $9.89 \pm 0.78$ | $11.06 \pm 0.21$ | – |
| 6 | *Aspergillus niger* | $8.96 \pm 0.05^{ab}$ | $9.69 \pm 0.81^{b}$ | $8.99 \pm 0.16^{ab}$ | $9.82 \pm 0.79$ | $10.95 \pm 0.93$ | – |
| 7 | *Botrytis cinerea Pers.* | $9.27 \pm 0.25^{ab}$ | $10.88 \pm 0.64$ | $9.39 \pm 0.68^{ab}$ | $10.89 \pm 1.08$ | $10.67 \pm 0.60$ | – |
| 8 | *Penicillium expansum* | $9.60 \pm 0.35^{ab}$ | $10.93 \pm 0.23$ | $9.14 \pm 1.30^{ab.}$ | $11.10 \pm 1.02$ | $10.6 \pm 0.87$ | – |

–No inhibition zone.

[a]The inhibitory effect on the same bacteria, which is statistically different between the 0.5 g group and the corresponding 1.0 g group ($p < 0.05$).

[b]The inhibitory effect on the same bacteria, which is statistically different from the positive control ($p < 0.05$). NC, negative control (normal saline); PC, 0.5 g/L positive control (streptomycin as positive control of bacteria and nystatin as positive control of fungi); SBP, sea buckthorn polysaccharide.

Table 2. Minimum Inhibitory Concentration of SBP Solutions and Film Solutions

| No. | Strain | MIC/SBP Concentration (g/L) | | | | | |
|---|---|---|---|---|---|---|---|
| | | 2 | 1 | 0.5 | 0.25 | 0.125 | 0.0625 |
| 1 | *Escherichia coli* | – | – | – | + | ++ | +++ |
| 2 | *Pseudomonas aeruginosa* | – | – | – | + | ++ | +++ |
| 3 | *Bacillus subtilis* | – | – | + | ++ | ++ | +++ |
| 4 | *Bacillus cereus* | – | – | + | ++ | ++ | +++ |
| 5 | *Aspergillus flavus* | – | – | – | + | ++ | ++ |
| 6 | *Aspergillus niger* | – | – | + | + | ++ | +++ |
| 7 | *Botrytis cinerea Pers.* | – | – | – | + | ++ | ++ |
| 8 | *Penicillium expansum* | – | – | – | + | ++ | ++ |

– No bacteria growth; + The growth of bacteria; SBP, sea buckthorn polysaccharide; MIC, minimum inhibitory concentration.

at 10,000 *g* at 4°C for 20 min. Then, 2 mL of the supernatant was reacted with 2 mL of 0.67% (w/v) thiobarbituric acid in a water bath for 20 min. After cooling to room temperature, the mixture was centrifuged again, and the absorbance of the supernatant was measured at 450 nm, 532 nm, and 600 nm. The control group used 2 mL of 100 g/L TCA solution instead of the supernatant (Zha et al., 2022). The malondialdehyde (MDA) content calculation utilized the total volume of the sample extraction solution ($V$), the volume taken for measurement ($V_S$), and the sample weight ($m$).

$$MDA\left({}^{\mu mol}/_{g}\, m_F\right) = \frac{[6.45\times(OD_{532}-OD_{600})-0.56\times OD_{450}]\times V}{V_S\times m\times 1000}$$

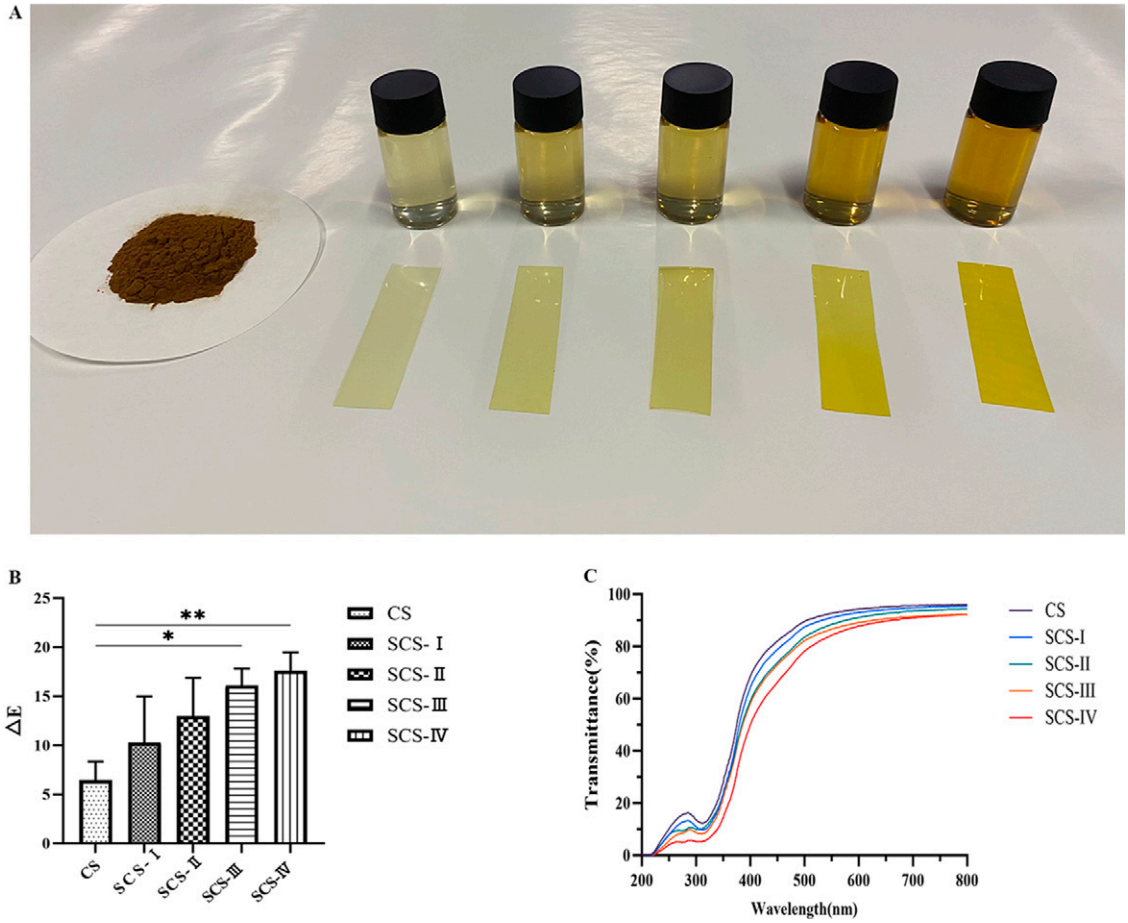


**FIG. 1.** The optical properties of composite films. **(A)** Physical images of SBP, film solution, and film. **(B)** The effect of different concentrations of SBP on the color of composite films. **(C)** The effect of different concentrations of SBP on the transmittance of composite films. The color of the column corresponds to different concentrations of composite films. Statistical difference between the two groups (*$p < 0.05$; **$p < 0.01$). Values are the average of three repeated determinations. The vertical bars represent the standard error. SBP, sea buckthorn polysaccharide.

*Statistical analysis*

Data analysis was conducted using GraphPad Prism version 10.0.2 software (San Diego, CA, United States). Results are expressed as means ± standard deviations. To assess the significance of differences among groups, one-way analysis of variance (ANOVA) was utilized. A $p$ value of <0.05 was considered to indicate statistical significance, whereas a $p$ value of <0.01 was deemed to indicate a significant difference. Visual representations of the data were created using both GraphPad Prism 10.0.2 and Photoshop 2020.

## Results and Discussion

*Optical properties of SCS composite films*

Color alteration. The integration of SBP into the SCS composite films significantly deepens the film color, an effect primarily attributable to the natural brown hue of SBP. There is a dose-dependent relationship between the amount of SBP incorporated and the ΔE value, indicating a substantial increase in total color difference (Fig. 1B). This color change corroborates visual assessments, highlighting the influence of SBP concentration on the esthetic properties of the SCS composite films.

*Opacity and UV resistance*

Opacity is a vital attribute for protecting food products from quality degradation caused by UV light exposure (Tripathi et al., 2023). The study demonstrates a decrease in light transmittance with increasing SBP concentration (Fig. 1C). This reduction in transmittance, reflecting the films' darker appearance as observed in Figure 1A, suggests improved UV-blocking capabilities of the SCS composite films, particularly for the SCS-IV variant, compared with the baseline chitosan film. Such enhanced UV resistance is crucial for extending the shelf life of light-sensitive food products by mitigating the rate of oxidation reactions.

*Physical properties of SCS composite films with SBP addition*

Swelling degree. The swelling degree (SD) serves as a predictive measure for the quality and stability of food products during storage. Notably, the incorporation of 100 mg/L SBP into the SCS films resulted in a lower SD compared with the CS films, with further reductions observed as SBP concentration increased (Fig. 2A). This phenomenon is attributed to the molecular interactions between CS and SBP, particularly the formation of hydrogen bonds and ionization of functional groups (Lian et al., 2020, Luo et al.,

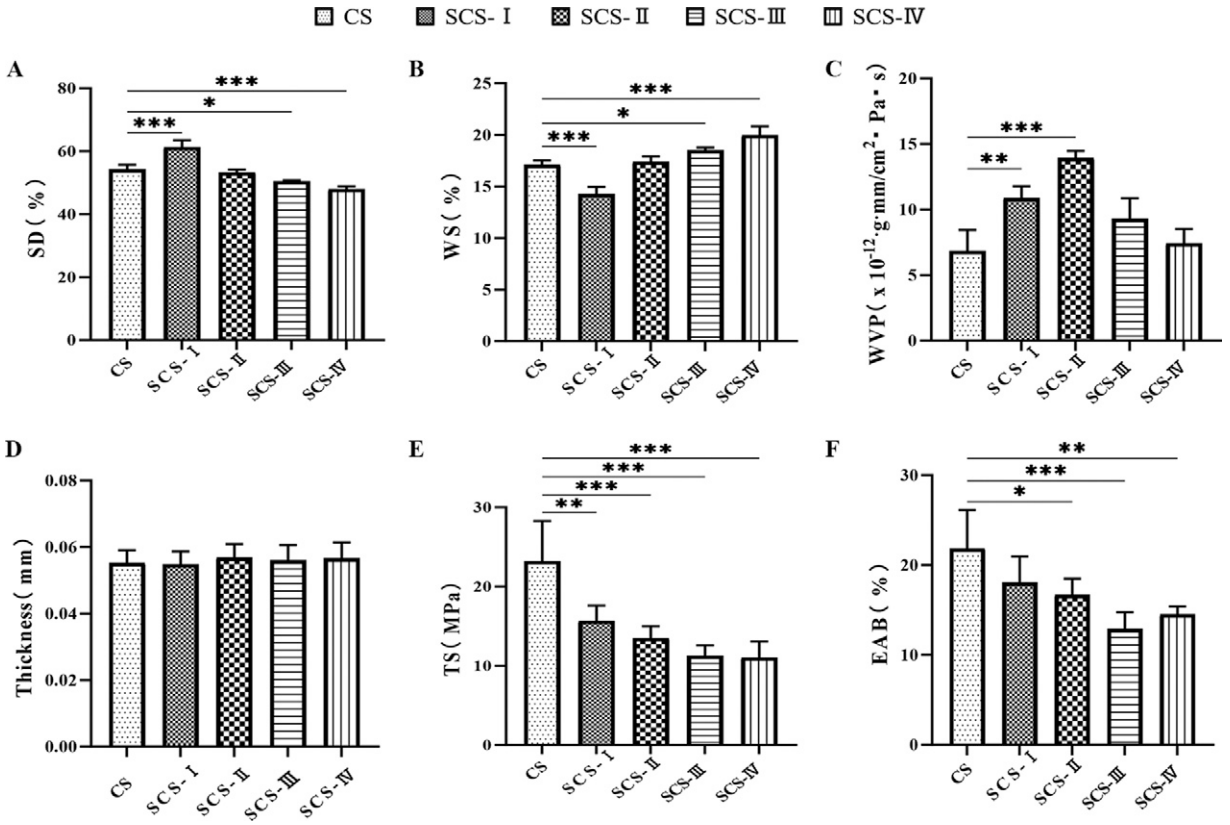


**FIG. 2.** The physical and mechanical properties of composite films. **(A)** The effect of different concentrations of SBP on the SD of composite films. **(B)** The effect of different concentrations of SBP on the WS of composite films. **(C)** The effect of different concentrations of SBP on the WVP of composite films. **(D)** The effect of different concentrations of SBP on the thickness of composite films. **(E)** The effect of different concentrations of SBP on the TS of composite films. **(F)** The effect of different concentrations of SBP on the EAB of composite films. The color of the column corresponds to different concentrations of composite films. Statistical difference between the two groups (*$p < 0.05$; **$p < 0.01$; ***$p < 0.001$). Values are the average of three repeated determinations. The vertical bars represent the standard error. SBP, sea buckthorn polysaccharide; SD, swelling degree; WS, water solubility; WVP, water vapor permeability; EAB, elongation at break; TS, tensile strength.

2021), which collectively reduce water molecule penetration into the film matrix.

Water solubility. The addition of SBP significantly influenced the water solubility (WS) of the SCS films and showed a dose-dependence (Fig. 2B), which is similar with the study by Al-Hilifi et al., 2023. The inherent hydrophilicity of SBP, due to its abundant -OH groups, facilitates the formation of hydrogen bonds with water molecules, resulting in a hydration layer that enhances the film's solubility. Moreover, increasing SBP concentrations lead to the extension of polysaccharide chains and exposure to more hydrophilic groups, further elevating the WS of the films.

Water vapor permeability. WVP is directly related to the film's ability to transfer moisture, which is paramount in determining the shelf life of packaged food (Dang et al., 2024). The study identified a pivotal concentration of 100 mg/L SBP, beyond which the WVP of the films exhibited a notable change (Fig. 2C). This shift is likely due to alterations in the molecular network density of the film, influenced by varying interactions among polysaccharide molecules at different SBP concentrations. Such findings indicate the potential of SBP concentration as a tunable factor for optimizing the moisture barrier properties of SCS films to meet specific food preservation needs.

### *Thickness and mechanical properties of SCS composite films*

As shown in Figure 2D, there is no significant difference in the thickness of all films ($p > 0.05$). The study observed that pure CS films exhibited the highest TS and EAB values (Fig. 2E–F), suggesting superior strength and flexibility. However, the addition of SBP resulted in a significant decrease in both TS and EAB of the SCS films (Lian et al., 2020). This reduction could be attributed to the predominant interaction among CS molecules over that between CS and SBP, leading to compromised mechanical properties.

### *Structural properties of SCS composite films*

FTIR analysis. FTIR spectral analysis of the CS films identified characteristic absorption peaks at 3353.05 $cm^{-1}$ and 2878.06 $cm^{-1}$ (Fig. 3A), indicative of the stretching vibrations of hydroxyl (-OH) and methylene (-CH) groups, respectively (Zeng et al., 2022). Notably, the absorption peak at 1564.18 $cm^{-1}$, associated with the -NH bending vibration, is significantly enhanced. In addition, a distinct peak at 1030.72 $cm^{-1}$, attributed to the antisymmetric stretching of C-O and the stretching of C-H bonds (Xiao et al., 2022), confirms the interaction between CS and SBP within the composite films.

### *SEM analysis*

SEM imaging elucidated the morphological distinctions between CS and SCS films. At lower concentrations, SBP integrates effectively with the CS solution, resulting in a uniform surface on the SCS composite films (Fig. 3B a–c). An increase in SBP concentration to 150 mg/L and 200 mg/L prompted an escalation in surface roughness and the emergence of bubbles within the SCS composite films (Fig. 3B d–e), aligning with

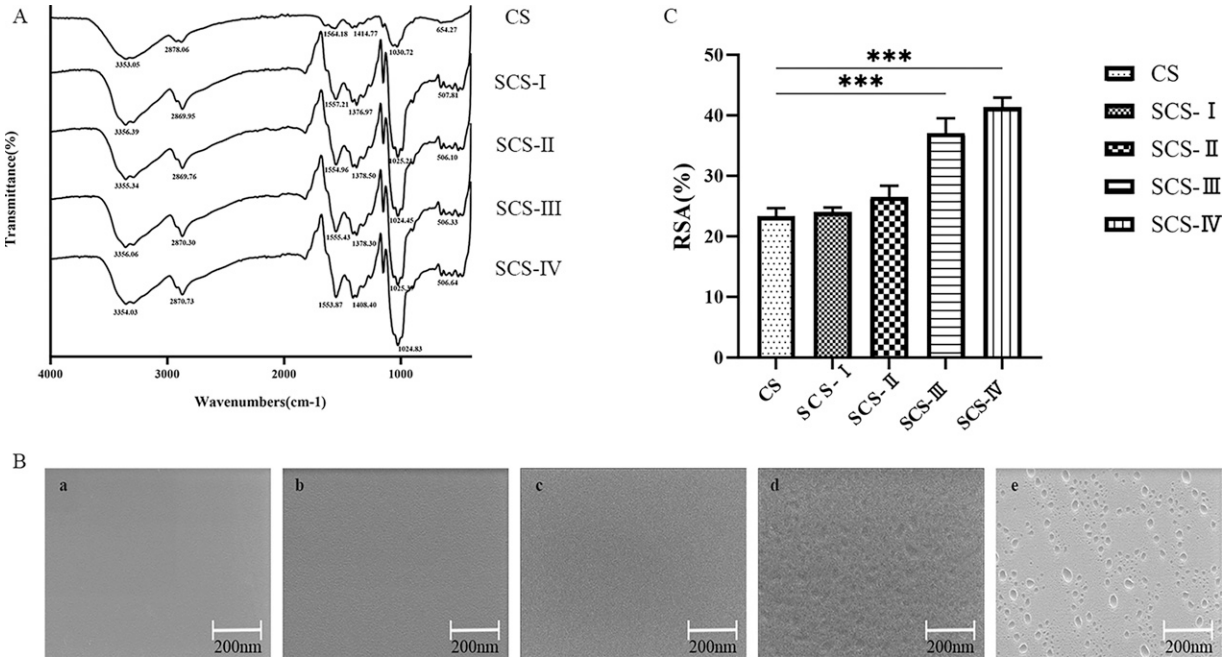


**FIG. 3.** The structure and antibacterial properties of composite films. **(A)** The effect of different concentrations of SBP on the ATR-FTIR image of composite films. **(B)** The effect of different concentrations of SBP on the SEM image of composite films. "a," "b," "c," "d," and "e" represents CS, SCS-I, SCS-II, SCS-III, and SCS-IV, respectively. **(C)** The effect of different concentrations of SBP on the DPPH free RSA of composite films. The color of the column corresponds to different concentrations of composite films. Statistical difference between the two groups (***$p < 0.001$). Values are the average of three repeated determinations. The vertical bars represent the standard error. SBP, sea buckthorn polysaccharide; ATR-FTIR, attenuated total reflectance Fourier transform infrared; SEM, scanning electron microscopy; CS, chitosan; SCS, chitosan/sea buckthorn polysaccharide; RSA, radical scavenging activity.

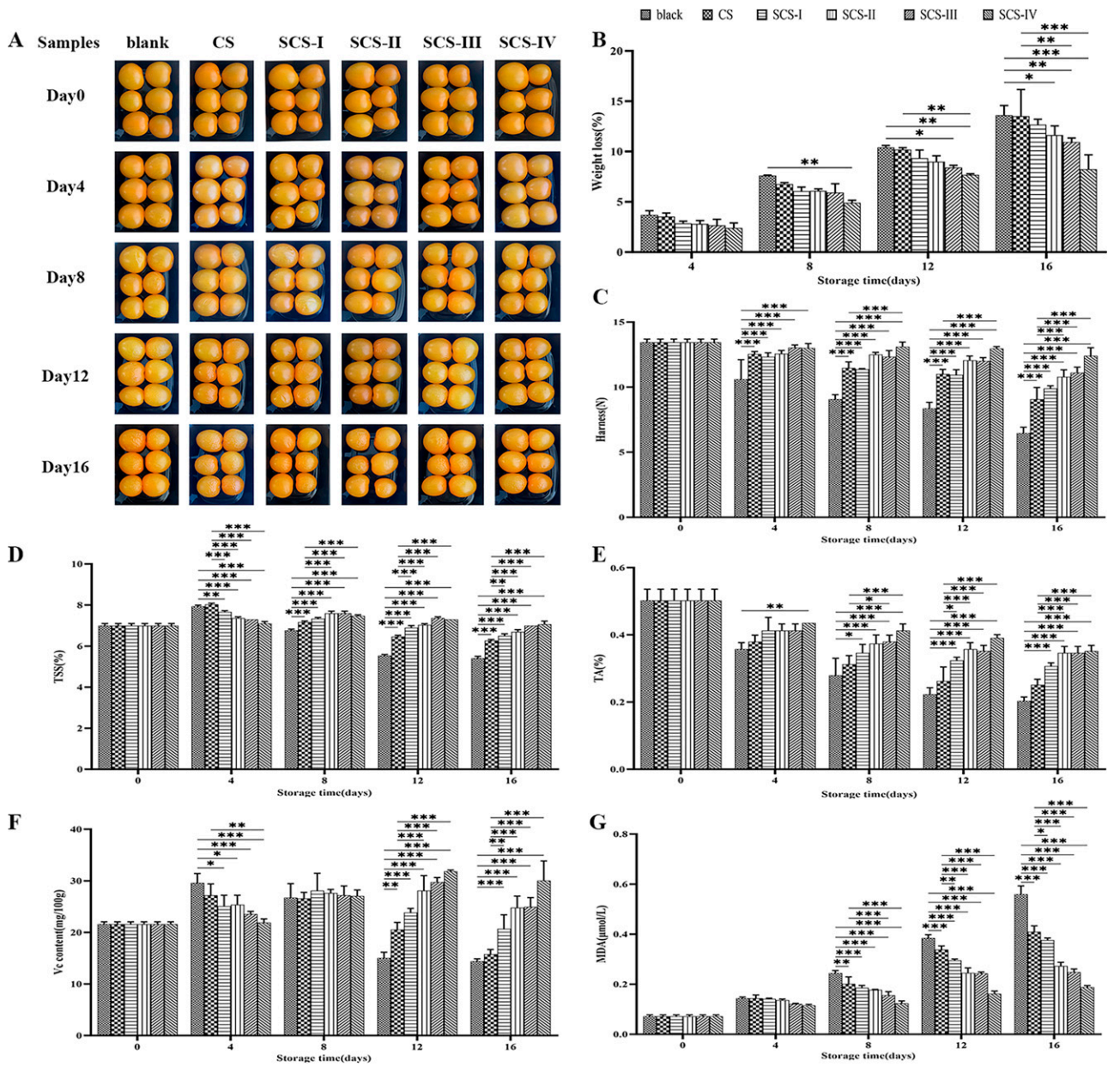


**FIG. 4.** Application of composite films in the preservation of yellow cherry tomatoes. **(A)** Appearance of yellow cherry tomatoes at different stages of storage. **(B)** The effect of different concentrations of SBP on the weight loss rate of yellow cherry tomatoes. **(C)** The effect of different concentrations of SBP on the hardness of yellow cherry tomatoes. **(D)** The effect of different concentrations of SBP on the TSS of yellow cherry tomatoes. **(E)** The effect of different concentrations of SBP on the TA of yellow cherry tomatoes. **(F)** The effect of different concentrations of SBP on the VC content of yellow cherry tomatoes. **(G)** The effect of different concentrations of SBP on the MDA of yellow cherry tomatoes. The effect of different concentrations of composite films on the yellow cherry tomatoes. The color of the column corresponds to different concentrations of composite films. Statistical difference between the two groups (*$p < 0.05$; **$p < 0.01$; ***$p < 0.001$). Values are the average of three repeated determinations. The vertical bars represent the standard error. SBP, sea buckthorn polysaccharide; TSS, total soluble solid; TA, titrable acid; MDA, malondialdehyde.

findings from previous studies on Chitosan/Whey Protein Hydrolysate Composite Films (Al-Hilifi et al., 2023).

### *DPPH free RSA*

The analysis demonstrated that SCS films exhibit superior antioxidant activity relative to pure CS films, with a direct correlation between SBP concentration and antioxidative capacity (Fig. 3C). This finding aligns with previous research (Zhao et al., 2023), highlighting the role of SBP in augmenting the antioxidant properties of the composite films.

### *Antimicrobial activity of SCS composite films enhanced by SBP addition*

The Oxford Cup method was used to evaluate the antimicrobial efficacy of varying concentrations of SBP in both solution form and as part of SCS composite films (Table 1).

The antimicrobial performance of SBP solutions and composite films increased concomitantly with increased SBP concentrations. At a concentration of 1 g/L of SBP, the solutions and films exhibited peak antibacterial activity, particularly against *Penicillium expansum*, highlighting the potent antimicrobial capacity of SBP at higher doses.

In Table 2, while SBP demonstrated significant inhibitory effects across a spectrum of microorganisms, its efficacy varied among different strains. For *Bacillus subtilis*, *Bacillus cereus*, and *Aspergillus niger*, the highest MIC was recorded at 1 g/L. Conversely, *Escherichia coli*, *Pseudomonas aeruginosa*, *Aspergillus flavus*, *Botrytis cinerea* Pers., and *Penicillium expansum* were more susceptible to SBP, showcasing the lowest MIC of 0.5 g/L. The findings indicate that by adjusting the concentration of SBP, SCS composite films could serve as an effective barrier against microbial spoilage, thereby extending the shelf life.

### *Effects of SCS composite films on preservation of yellow cherry tomatoes*

On the 8th day of storage, tomatoes packaged in SCS composite films exhibited less wrinkling and maintained a smoother appearance compared with those in the blank and pure CS groups (Fig. 4A). This trend of reduced weight loss was particularly pronounced in samples treated with 150 and 200 mg/L SBP, demonstrating a statistically significant preservation effect ($p < 0.01$) by the 16th day of storage (Fig. 4B). At the same time period, as the SBP content increased, the hardness increased. Furthermore, the hardness measurements indicated that the composite films effectively mitigated softening (Zhao et al., 2023), suggesting a protective role against respiration metabolism and water loss (Fig. 4C). The content of TSS and TA are critical indicators of fruit maturity and flavor profile (Pasha et al., 2023). Throughout a 16-day storage period, the TSS of tomatoes first increased, then decreased, reflecting a natural ripening process influenced by storage conditions (Fig. 4D). The TA levels similarly declined over time, with the most significant drop observed in samples without film coverage (Fig. 4E), which is similar to the results reported in other coating literature (Al-Hilifi et al., 2022). This may be due to the limitations of fruit respiration rate and water loss. However, the application of SCS composite films (Roshandel-Hesari et al., 2022), especially those with 200 mg/L SBP, effectively moderated these changes, indicating a superior preservation effect. Tomatoes covered with SCS films showed an initial increase in VC, followed by a decrease, diverging from the trend observed in the blank group (Fig. 4F). This pattern suggests that SCS composite films can protect VC from oxidation and degradation, with the highest SBP concentration providing the most significant protective effect (Zhao et al., 2023). MDA content peaked by the 16th day across all groups. However, the accumulation of MDA was notably lower in tomatoes treated with SBP, with the lowest levels observed in the SCS-IV group (Fig. 4G). This reduction in MDA content underscores the effectiveness of SBP in enhancing fruit quality during storage (Zha et al., 2022).

## Conclusion

In conclusion, the integration of SBP into CS films significantly enhances their structural and antioxidative characteristics, while also inducing notable changes in surface morphology and mechanical integrity. Films containing 200 mg/L of SBP have shown increased antibacterial efficacy and considerable preservation capabilities for yellow cherry tomatoes, highlighting the potential of SCS composite films to extend the shelf life and maintain the quality of perishable fruits and vegetables. Despite improvements in UV resistance, WS, and antioxidant activity, the films still require refinement in areas such as hydrophobicity and mechanical strength. Future research will focus on addressing these limitations and expanding the applicability and performance of SBP-based composite films within food preservation technologies.

## Authors' Contributions

M.X.: composite films preparation experiment, fresh-keeping test methodology, data analysis, writing—original draft, and modification. A.S.: composite films preparation experiment, fresh-keeping test methodology, data analysis, and modification. X.C.: Fresh-keeping test methodology and modification. T.L. and J.Z.: Data analysis and modification. S.L.: Antibacterial test methodology, data analysis, and modification. W.Y.: Funding acquisition, writing—original draft, data analysis, and modification. All authors have read and agreed to the published version of the article.

## Disclosure Statement

The authors have declared no conflicts of interest for this article.

## Funding Information

This work was supported by the Natural Science Foundation of Liaoning Province (2018010874–301, 2017225065) and Shenyang Medical College Scientific Research Innovation Fund (20182033, 20191038).

## References

Al-Hilifi SA, Al-Ali RM, Al-Ibresam OT, et al. Physicochemical, morphological, and functional characterization of edible anthocyanin-enriched *Aloevera* coatings on fresh figs (*Ficus carica* L.). Gels 2022;8(10):645; doi: 10.3390/gels8100645

Al-Hilifi SA, Al-Ali RM, Dinh LNM, et al. Development of hyaluronic acid based polysaccharide-protein composite edible coatings for preservation of strawberry fruit. Int J Biol Macromol 2024;259(Pt 1):128932; doi: 10.1016/j.ijbiomac.2023.128932

Al-Hilifi SA, Al-Ibresam OT, Al-Hatim RR, et al. Development of chitosan/whey protein hydrolysate composite films for food packaging application. J Compos Sci 2023;7(3):94; doi: 10.3390/jcs7030094

Bai Y, Zhao Y, Li Y, et al. UV-shielding alginate films crosslinked with Fe3+ containing EDTA. Carbohydr Polym 2020; 239:115480; doi: 10.1016/j.carbpol.2019.115480

Dang X, Du Y, Wang X. Engineering eco-friendly and biodegradable biomass-based multifunction al antibacterial packaging films for sustainable food preservation. Food Chem 2024;439:138119; doi: 10.1016/j.foodchem.2023.138119

Kaczmarek-Szczepańska B, Zasada L, Grabska-Zielińska S. The physicochemical, antioxidant, and color properties of thin films based on chitosan modified by different phenolic acids. Coatings 2022;12(2):126; doi: 10.3390/coatings12020126

Kumar N, Petkoska AT, Al-Hilifi SA, et al. Effect of chitosan–pullulan composite edible coating functionalized with pomegranate peel extract on the shelf life of mango (*Mangifera indica*). Coatings 2021;11(7):764; doi: 10.3390/coatings11070764

Kumar S, Mukherjee A, Dutta J. Chitosan based nanocomposite films and coatings: Emerging antimicrobial food packaging alternatives. Trends in Food Science & Technology 2020;97: 196–209; doi: 10.1016/j.tifs.2020.01.002

Li Q, Dou Z, Duan Q, et al. A comparison study on structure-function relationship of polysaccharides obtained from sea buckthorn berries using different methods: Antioxidant and bile acid-binding capacity. Food Science and Human Wellness 2024;13(1):494–505; doi: 10.26599/FSHW.2022.9250043

Lian H, Shi J, Zhang X, et al. Effect of the added polysaccharide on the release of thyme essential oil and structure properties of chitosan based film. Food Packaging and Shelf Life 2020; 23:100467; doi: 10.1016/j.fpsl.2020.100467

Liu J, Liu S, Wu Q, et al. Effect of protocatechuic acid incorporation on the physical, mechanical, structural and antioxidant properties of chitosan film. Food Hydrocolloids 2017;73: 90–100; doi: 10.1016/j.foodhyd.2017.06.035

Liu J, Xu D, Chen S, et al. Superfruits in China: Bioactive phytochemicals and their potential health benefits—A review. Food Sci Nutr 2021;9(12):6892–6902; doi: 10.1002/fsn3.2614

Luo A, Hu B, Feng J, et al. Preparation, and physicochemical and biological evaluation of chitosan-*Arthrospira platensis* polysaccharide active films for food packaging. J Food Sci 2021;86(3):987–995; doi: 10.1111/1750-3841.15639

Marangoni Júnior L, Jamróz E, Gonçalves S, et al. Preparation and characterization of sodium alginate films with propolis extract and nano-SiO2. Food Hydrocolloids for Health 2022; 2:100094; doi: 10.1016/j.fhfh.2022.100094

Narasagoudr SS, Hegde VG, Vanjeri VN, et al. Ethyl vanillin incorporated chitosan/poly(vinyl alcohol) active films for food packaging applications. Carbohydr Polym 2020;236: 116049; doi: 10.1016/j.carbpol.2020.116049

Pasha HY, Mohtasebi SS, Tajeddin B, et al. The effect of a new bionanocomposite packaging film on postharvest quality of strawberry at modified atmosphere condition. Food Bioprocess Technol 2023;16(6):1246–1257; doi: 10.1007/s11947-022-02968-0

Roshandel-Hesari N, Mokaber-Esfahani M, Taleghani A, et al. Investigation of physicochemical properties, antimicrobial and antioxidant activity of edible films based on chitosan/casein containing *Origanum vulgare* L. essential oil and its effect on quality maintenance of cherry tomato. Food Chem 2022;396:133650; doi: 10.1016/j.foodchem.2022.133650

Roy S, Rhim J-W. Effect of CuS reinforcement on the mechanical, water vapor barrier, UV-light barrier, and antibacterial properties of alginate-based composite films. Int J Biol Macromol 2020;164:37–44; doi: 10.1016/j.ijbiomac.2020.07.092

Shariatinia Z. Carboxymethyl chitosan: Properties and biomedical applications. Int J Biol Macromol 2018;120(Pt B): 1406–1419; doi: 10.1016/j.ijbiomac.2018.09.131

Shen A, Zhang T, Li S, et al. Beneficial effects of *Pleurotus citrinopileatus* polysaccharide on the quality of cherry tomatoes during storage. Foodborne Pathog Dis 2023;20(9):398–404; doi: 10.1089/fpd.2023.0032

Shen C, Wang T, Guo F, et al. Structural characterization and intestinal protection activity of poly saccharides from Sea buckthorn (Hippophae rhamnoides L.) berries. Carbohydr Polym 2021;274:118648; doi: 10.1016/j.carbpol.2021.118648

Sun J, Li Y, Cao X, et al. A film of chitosan blended with ginseng residue polysaccharides as an antioxidant packaging for prolonging the shelf life of fresh-cut melon. Coatings 2022; 12(4):468; doi: 10.3390/coatings12040468

Tripathi S, Kumar L, Deshmukh RK, et al. Ultraviolet blocking films for food packaging applications. Food Bioprocess Technol 2023;17(6):1563–1582; doi: 10.1007/s11947-023-03221-y

Wu J, Song G, Huang R, et al. Fish gelatin films incorporated with cinnamaldehyde and its sulfobutyl ether-$\beta$-cyclodextrin inclusion complex and their application in fish preservation. Food Chem 2023;418:135871; doi: 10.1016/j.foodchem.2023.135871

Xiao L, Kang S, Lapu M, et al. Preparation and characterization of chitosan/pullulan film loading carvacrol for targeted antibacterial packaging of chilled meat. Int J Biol Macromol 2022;211:140–149; doi: 10.1016/j.ijbiomac.2022.05.044

Zeng Y, Wang Y, Tang J, et al. Preparation of sodium alginate/-konjac glucomannan active films containing lycopene microcapsules and the effects of these films on sweet cherry preservation. Int J Biol Macromol 2022;215:67–78; doi: 10.1016/j.ijbiomac.2022.06.085

Zha Z, Tang R, Wang C, et al. Riboflavin inhibits browning of fresh-cut apples by repressing phenolic metabolism and enhancing antioxidant system. Postharvest Biology and Technology 2022;187:111867; doi: 10.1016/j.postharvbio.2022.111867

Zhao J, Wang Y, Li J, et al. Preparation of chitosan/Enoki mushroom foot polysaccharide composite c ling film and its application in blueberry preservation. Int J Biol Macromol 2023;246:125567; doi: 10.1016/j.ijbiomac.2023.125567

Address correspondence to:
*Weiwei Yang, PhD*
*Department of Food Science*
*College of Public Health*
*Shenyang Medical College*
*Shenyang*
*110034*
*China*

*E-mail:* yangweiwei@symc.edu.cn